Electronic Supplementary Material (ESI) for Nanoscale.

Magnetic/NIR-responsive drug carrier, multicolor cell imaging, and enhanced photothermal therapy of gold capped magnetite-fluorescent carbon hybrid nanoparticles

Hui Wang [a], Guixin Cao [b], Zheng Gai [b], Kunlun Hong [b], Probal Banerjee [a], Shuiqin Zhou[a*]

[a] *Department of Chemistry of College of Staten Island and The Graduate Center, The City University of New York, Staten Island, NY 10314, USA*
[b]*Center for Nanophase Materials Sciences and Chemical Science Division, Oak Ridge National Laboratory, Oak Ridge, TN 37831, USA*

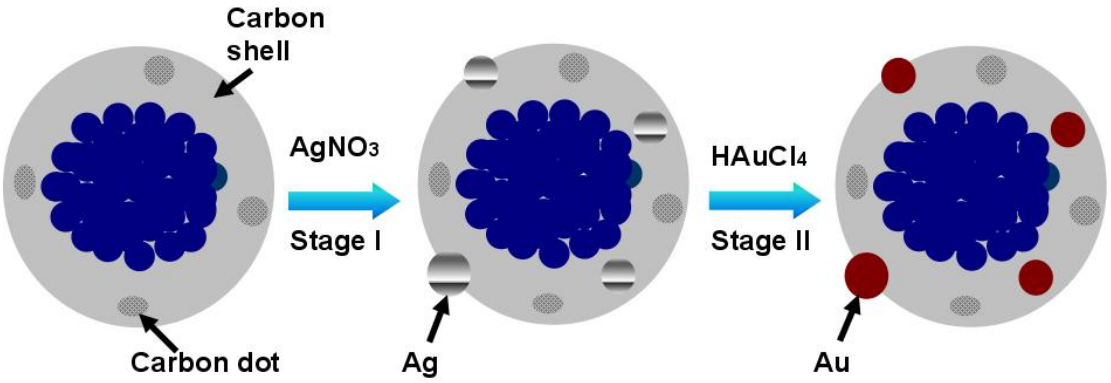

Figure S1. Synthetic process of multifunctional Fe_3O_4@PC-CDs-Au NPs. Stage I: formation of Fe_3O_4@PC-CDs-Ag NPs by the loading and reduction of Ag^+; Stage II: formation of Fe_3O_4@PC-CDs-Au NPs by the galvanic replacement reaction between the Au precursor ($HAuCl_4$) and Ag nanocrystals.

Department of Chemistry of College of Staten Island and The Graduate Center, The City University of New York, Staten Island, NY 10314, USA
E-mail address: shuiqin.zhou@csi.cuny.edu (S. Zhou); Tel.: +1 718 982 3897; Fax: +1 718 982 3910.

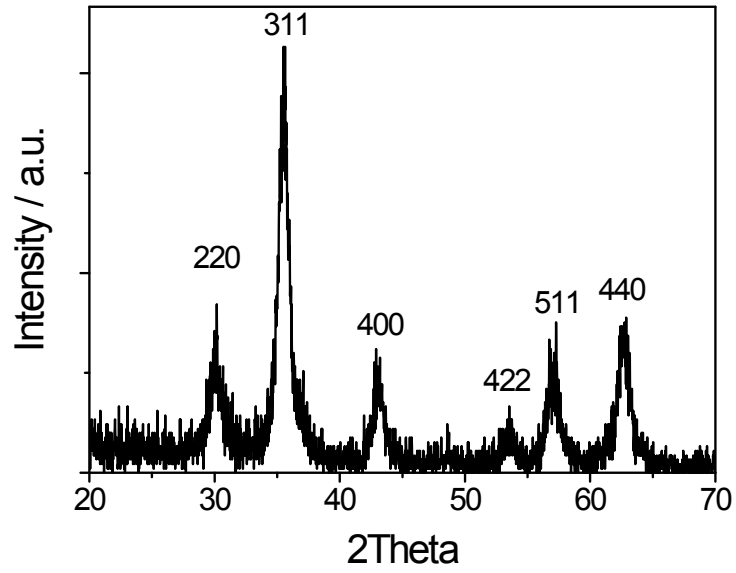

Figure S2. Typical XRD pattern of the as-obtained Fe_3O_4@PC-CDs NPs.

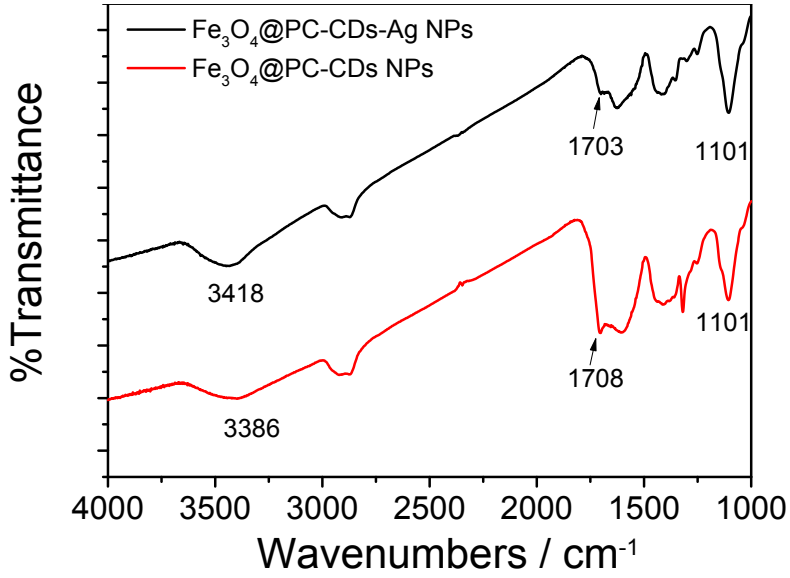

Figure S3. FT-IR spectra of the Fe_3O_4@PC-CDs and Fe_3O_4@PC-CDs-Ag hybrid NPs.

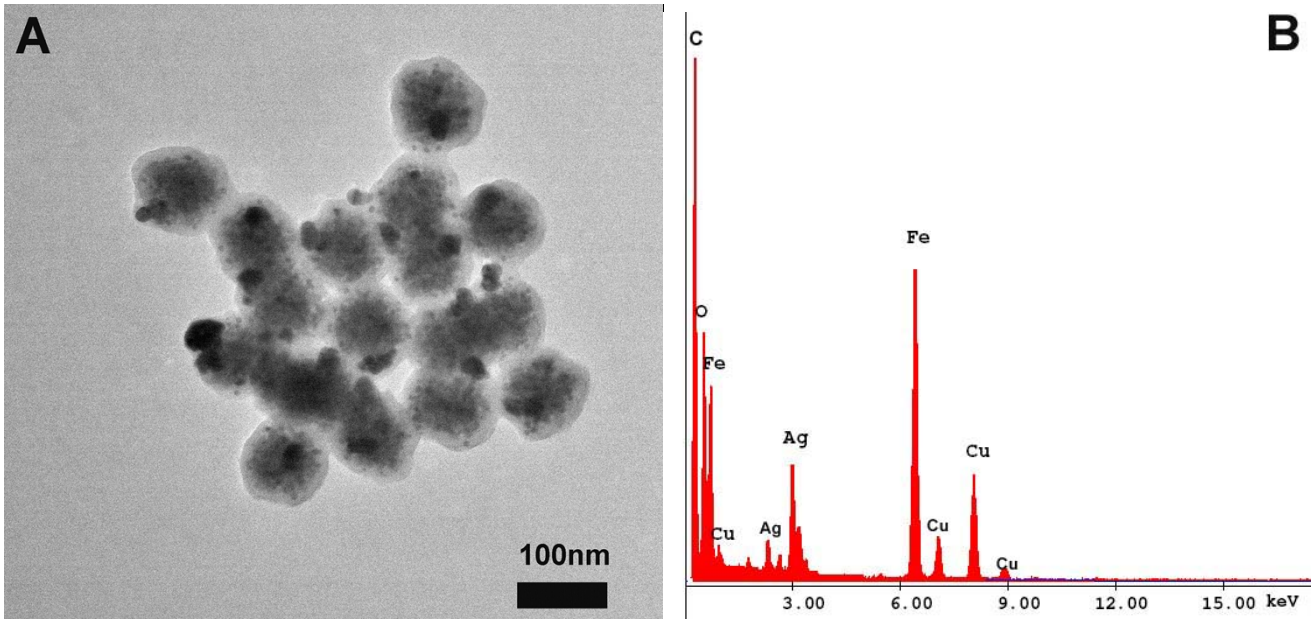

Figure S4. (A) TEM image of the as-obtained Fe_3O_4@PC-CDs-Ag NPs ;(B) EDAX of the single Fe_3O_4@PC-CDs-Ag NP.

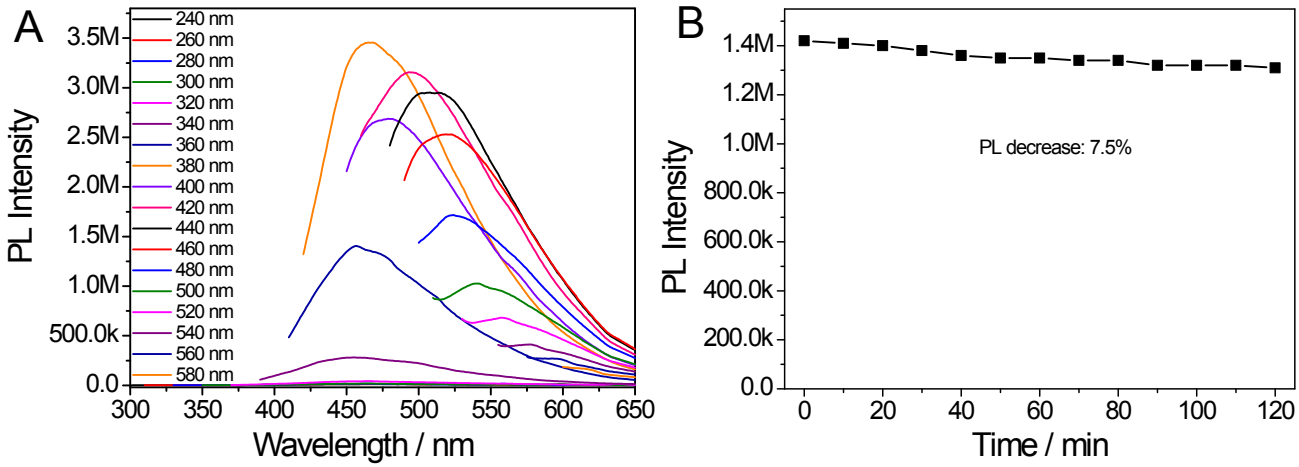

Figure S5. (A) PL spectra of the Fe_3O_4@PC-CDs-Au NPs at different excitation wavelengths. (B) Time dependent PL intensity variation (7.5%) of the Fe_3O_4@PC-CDs-Au NPs under a 2h continuous exposure to the excitation UV light of 365 nm.

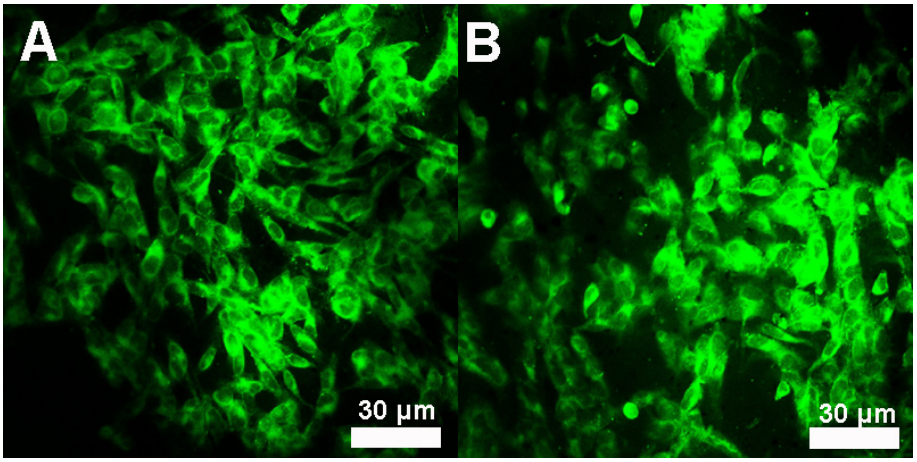

Figure S6. Laser scanning confocal microscopy images of B16F10 cells incubated with (A) Fe_3O_4@PC-CDs NPs and (B) Fe_3O_4@PC-CDs-Ag NPs under a excitation wavelengths of 488nm.

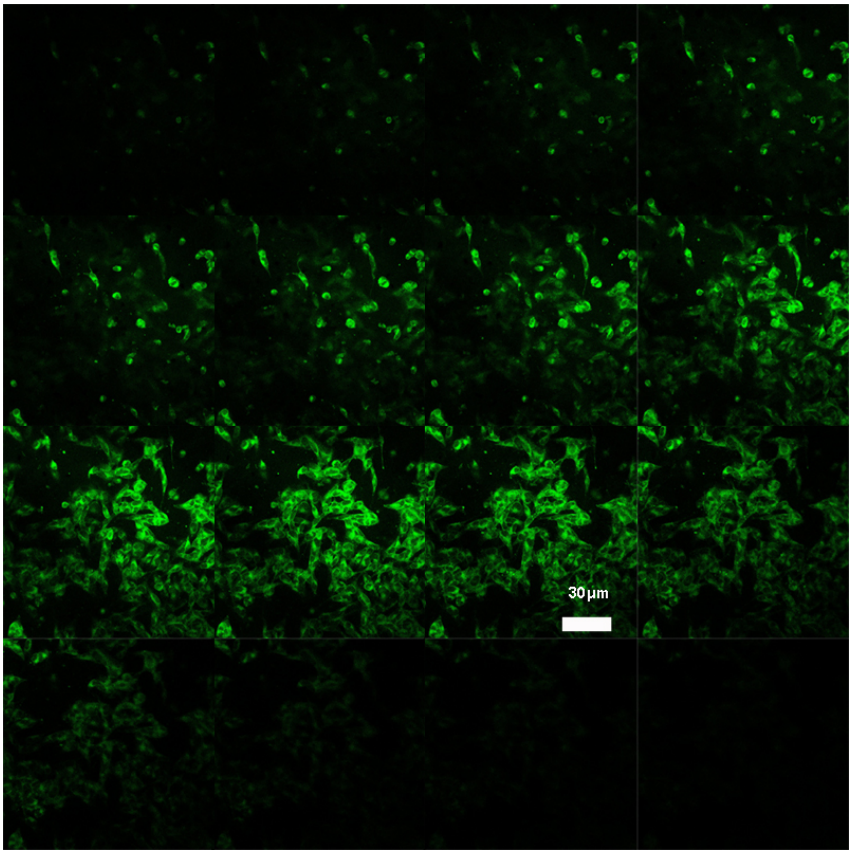

Figure S7. Z-Scanning confocal fluorescence transmission images of mouse melanoma cells B16F10 incubated with Fe_3O_4@PC-CDs-Au NPs.

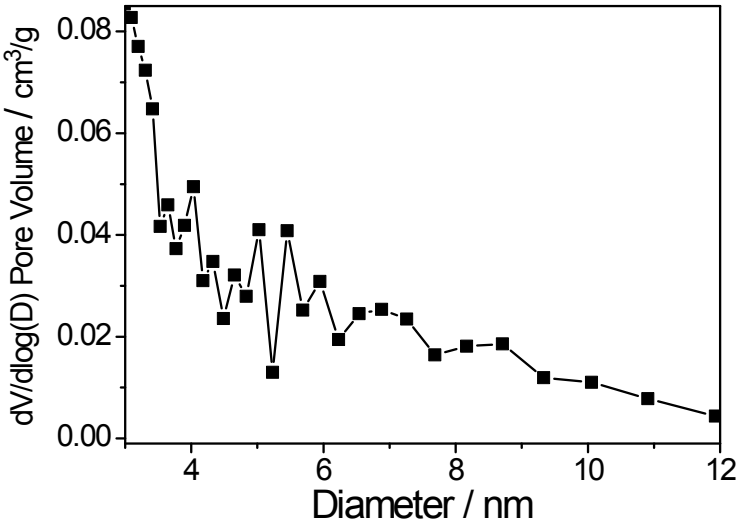

Figure S8. The pore size distribution of the as-obtained Fe_3O_4@PC-CDs-Au NPs.

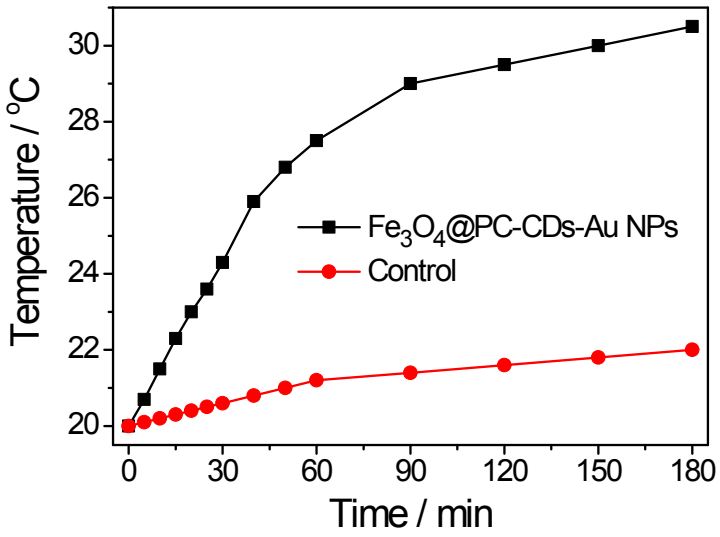

Figure S9. Hyperthermia assay on aqueous dispersion of Fe_3O_4@PC-CDs-Au NPs (0.01 g/L) and water (control) under an alternating magnetic field.

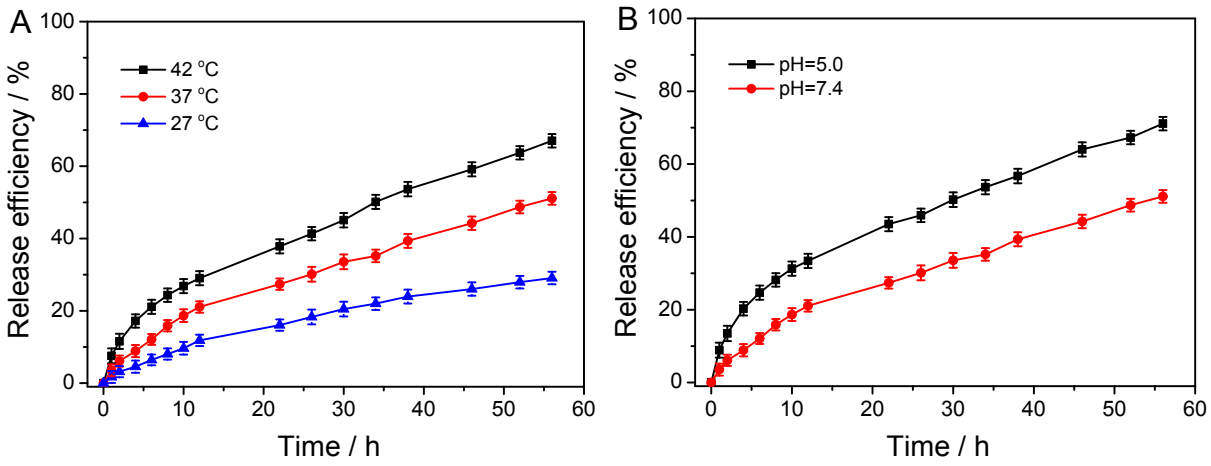

Figure S10. (A) Releasing profiles of DOX from the Fe_3O_4@PC-CDs-Au NPs at pH=7.4 under different temperatures of 27 ºC, 37 ºC, and 42 ºC, respectively. (B) Releasing profiles of DOX from the Fe_3O_4@PC-CDs-Au NPs in buffer solutions of different pH of 5.0 and 7.4, respectively, at 37 ºC.

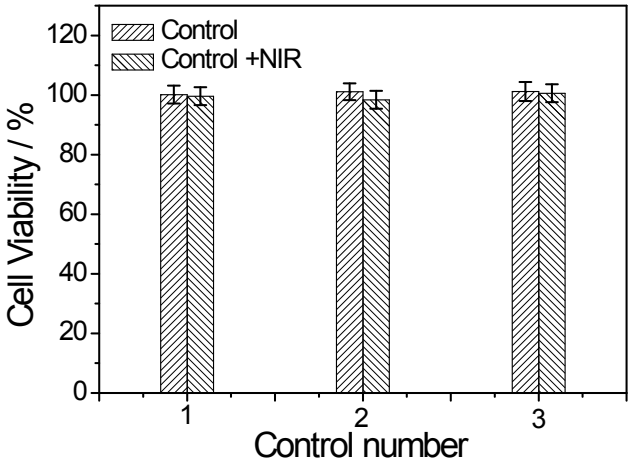

Figure S11. In vitro cell viability in the control culture medium without/with 1.5 W/cm^2 NIR irradiation for 5 min.

m^2.